Available online at www.sciencedirect.com
ScienceDirect
Chemical Physics 348 (2008) 45–52
Chemical Physics
www.elsevier.com/locate/chemphys

Nonlinear optical properties of pyridinium-betaines of squaric acid: Experimental and theoretical study

Tsonko M. Kolev [a,*], Denitsa Y. Yancheva [a], Bistra A. Stamboliyska [a], Momtchil D. Dimitrov [a], Rüdiger Wortmann [b,1]

[a] Institute of Organic Chemistry, Bulgarian Academy of Sciences, 1113 Sofia, Bulgaria
[b] Department of Physical Chemistry, Technical University of Kaiserslautern, 67663 Kaiserslautern, Germany

Received 7 December 2007; accepted 12 February 2008
Available online 15 February 2008

Abstract

The linear and nonlinear optical properties of six pyridinium-betaines of squaric acid were characterized by means of electro-optical absorption measurements (EOAM) in dioxane solution. All chromophores studied exhibit intense absorption bands in the visible region within 372–441 nm, accompanied with decrease in dipole moment upon excitation. The static hyperpolarizabilities of the NLO-phores studied depend strongly on the substituent in the pyridinium ring and increase significantly going from donor to acceptor substituent. Specifically, the noncentrosymmetrically crystallizing 4-benzoyl compound showed the highest static hyperpolarizability. These empirical trends were supported and verified by quantum-chemical calculations (DFT and *ab initio* RHF). Bulk crystal properties such as decomposition points within the high temperature range 480–665 K and improved thermal stability in melt demonstrate the advantage of these materials for nonlinear optical applications.

Keywords: Organic materials for nonlinear optics; EOAM; UV–vis; Molecular design; DFT

1. Introduction

Modern information technology requires new methods for data processing, fast optical data transfer and high-density storage of the acquired data. One approach to meet this goal is the development of new highly efficient organic materials with non-linear optical properties (NLO-phores). The group of materials introduced so far comprises poled polymers, guest-host systems, single-crystal materials, organic glasses, etc. [1–4].

The nonlinear optical efficiency of organic materials is affected by the nature of the conjugated bonds, the strength of the donor and acceptor groups and the molecular conformations. The main classes of organic compounds with different configurations are described in the literature [1–5]: 1D (dipolar compounds) like 4-nitroaniline; 2D (quadrupolar or Λ-shaped compounds) like 4,6-dinitroresorcinol; and 3D (octupolar compounds) like 1,3,5-triamino-2,4,6-trinitrobenzene. When considering the simplest case of 1D NLO-phores, a two-level model can be used for description of the second-order molecular nonlinearity (β) [1,2]. β can be expressed in terms of difference between ground- and excited-state dipole moments ($\Delta\mu_{ag}$), transition dipole moment (μ_{ag}) and HOMO–LUMO energy band gap (ΔE) of the occurring charge-transfer (CT) according Eq. (1), based on the Taylor series convention

$$\beta_0 = \frac{6\Delta\mu_{ag}(\mu_{ag})^2}{(\Delta E)^2} \quad (1)$$

The second-order molecular nonlinearity associated with a single chromophore will lead to observable bulk second-order nonlinearity (χ^2) only if the individual chromophores are oriented in a noncentrosymmetric manner.

* Corresponding author. Tel.: +359 2 9606106; fax: +359 2 8700225.
E-mail address: kolev@orgchm.bas.bg (T.M. Kolev).
[1] Deceased, 13 March 2005.

0301-0104/$ - see front matter © 2008 Elsevier B.V. All rights reserved.
doi:10.1016/j.chemphys.2008.02.018

The appropriate chromophore alignment can be achieved by covalent bonding to poled polymers [6–8], or molecular self-assembly by crystal growth, incorporation into inclusion compounds, and formation of liquid crystal domains [9,10]. However, since the long-term orientational stability of the acentric arrangement in poled polymers is limited, the single-crystal materials offer distinctive advantages for achieving the noncentrosymmetric alignment. Their higher chromophore density and improved thermal stability [11–13] comprise important features for practical use as NLO materials.

By applying the crystal engineering strategies for design of noncentrosymmetrical single-crystal NLO materials some new highly efficient frequency doublers have been already developed. The properly substituted cyclobutenediones proved to be excellent electron acceptors and certain squaric acid derivatives exhibited high NLO responses [14–18]. Following this approach, we have studied pyridinium-betaines of the squaric acid for their spectral and structural properties. Valuable information on their spectral behaviour, molecular and crystal structure was obtained by means of UV–vis [19], IR [20–22] and X-ray [23–28] methods. All applied techniques indicate the pyridinium-betaines as a promising new class of organic zwitterionic NLO-phores. However, to the best of our knowledge, their second-order NLO properties have not been reported yet.

Thus the present contribution focuses on the electro-optical absorption measurements (EOAM) for six donor and acceptor substituted (labeled **3a–f**) pyridinium-betaines of squaric acid. We used also density functional theory (DFT) and *ab initio* RHF calculations in order to perform structural analysis of the studied molecules and to predict their optical and non-linear optical properties. The comparison with the experimental EOAM data provides important information on the ability of these computational methods to describe the NLO characteristics. Having in mind, that one of the challenges in the design of new NLO materials is to achieve high optical nonlinearity and good thermal stability in one compound, finally we have investigated the decomposition temperatures and the thermal stability in melt by a TG–DTG analysis.

2. Experimental and computational details

The condensation of squaric acid (**1**, Scheme. 1) with equimolar amounts of substituted pyridines (**2**, Scheme. 1) in acetic anhydride affords as products the corresponding pyridinium-betaines of squaric acid (**3a–f**, Scheme. 1). The general procedure applied is according to Schmidt [29] and it was previously described by us in detail [19].

Absorption spectra were recorded with a Perkin–Elmer Lambda 900 Spectrometer at 298 K (scan speed of 100 nm min^{-1}, 3 cm quartz glass cuvette).

The EOA measurements were carried out applying the standard equipment of EOA spectroscopy as described with all details in Refs. [1,2,30,31]. The EOAM experiment was performed in 1,4-dioxane solution with chromophore concentration of 10^{-5} mol l^{-1}. The technique has been established as efficient tool for screening of molecular parameters such as ground-state dipole moments (μ_g), difference between the ground- and excited-state dipoles ($\Delta\mu_{ag} = \mu_a - \mu_g$) and transition dipole moment (μ_{ag}) of the occurring charge-transfer (CT). On the basis of these quantities a subsequent estimation of the static hyperpolarizabilities β_0(exp) of the chromophores was made within the two-level model [30,31].

The TG–DTG (thermogravimetric analysis) investigations were performed on a Setaram TG92 instrument. Samples of 20 mg were placed in a microbalance crucible and heated in an Ar flow (70 cm^3 min^{-1}) up to 523 or 623 K at 5 K min^{-1}.

The quantum chemical calculations were performed with GAUSSIAN-98 program package [32]. The geometry optimizations were carried out by the DFT method, using Becke's three-parameter hybrid exchange functional combined with Lee–Yang–Parr correlation functional (B3LYP) [33,34] with the 6-311G(d,p) basis set. Molecular hyperpolarizabilities at zero frequency were calculated by Coupled Perturbed Hartree-Foch (CPHF) at HF/6-311G** level of theory and the default parameters provided by the polar keywords. The averaged polarizabilities (α), first hyperpolarizabilities ($\beta_{0,tot}$) and its component along the dipole axis ($\beta_{0,vec}$) given in this paper were obtained according to the following equations:

$$\mu_g = (\mu_x^2 + \mu_y^2 + \mu_z^2)^{1/2} \tag{2}$$

$$\alpha = \frac{1}{3}(\alpha_{xx} + \alpha_{yy} + \alpha_{zz}) \tag{3}$$

$$\beta_i = \sum_j \beta_{ijj} \tag{4}$$

$$\beta_{0,tot} = (\beta_x^2 + \beta_y^2 + \beta_z^2)^{1/2} \tag{5}$$

$$\beta_{0,vec} = \frac{\mu_x\beta_x + \mu_y\beta_y + \mu_z\beta_z}{|\mu_g|} \tag{6}$$

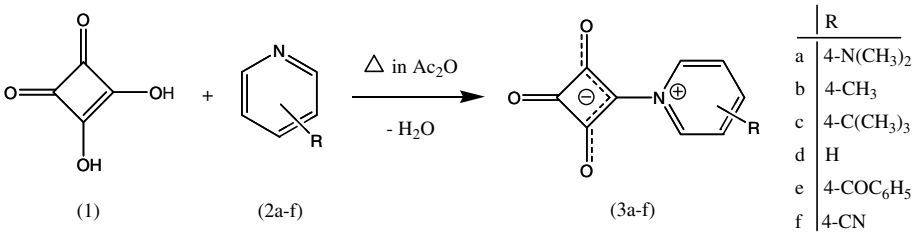

Scheme 1. Synthetic scheme for preparation of pyridinium-betaines of squaric acid **3a–f**. R is the substituent type.

The static first hyperpolarizabilities β_0 were calculated according to the Taylor convention used in the EOA measurements in order to be consistent with the experimental data [35].

3. Results and discussion

3.1. Optical properties

As usually observed for 1D NLO-phores [1–4], each of the chromophores **3a–f** used in this study displays a strong CT absorption band in the visible region of the UV spectrum. The absorption maxima (λ_{ag}) of all compounds in 1,4-dioxane and acetonitrile are listed in Table 1. UV–vis absorption spectra of some representative derivatives in acetonitrile are illustrated in Fig. 1.

λ_{ag} is within the 362–419 nm range in acetonitrile, and 372–441 nm in 1,4-dioxane (Table 1) and depends on the medium polarity and the substituent nature. The occurrence of a strong CT in **3a–f** is evidenced by the high coplanarity between the squaric and pyridine rings. In both solvents the absorption maxima shift bathochromically going from donor to acceptor substituted species. The presence of donor groups ($N(CH_3)_{2-}$, $C(CH_3)_{3-}$, and CH_{3-}) in the pyridinium ring only slightly affects the band position and λ_{ag} is nearly constant for **3a–c** (Table 1). In contrast, the presence of acceptor groups (CN and COC_6H_5) leads to more than 30 nm red shift (**3e–f**) as compared to the unsubstituted compound **3d**. The introduction of donor substituents in the pyridinium ring appears to increase the dipolar ground-state structure, whereas, acceptor groups reduce it and favour the CT excitation.

The dependence of the CT band on the medium polarity manifests itself through a pronounced negative solvatochromism (Table 1). This is typical for structures strongly polarized in ground state and characterized by reverse CT though excitation [19,22,36]. In the UV spectra of the compounds with donor substituents the negative solvatochromism is not so strongly expressed and the hypsochromic shift of the absorption maxima in the more polar solvent acetonitrile is only *ca.* 10 nm for **3a–c** (Table 1), whereas this shift for **3e** and **3f** is *ca.* 20 nm.

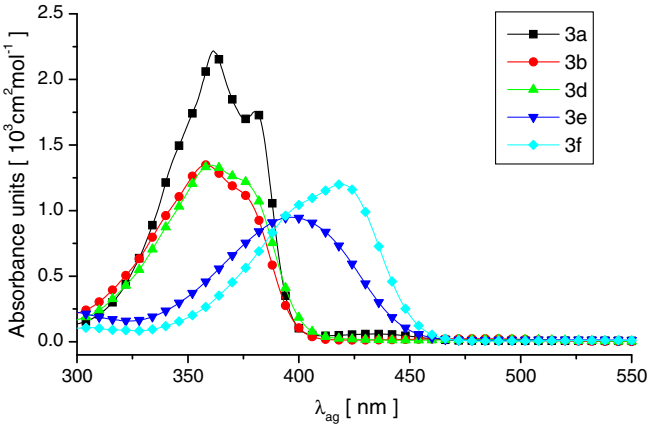

Fig. 1. UV–vis absorption spectra of some pyridinium-betaines of squaric acid in acetonitrile, $T = 298$ K.

3.2. Electro-optical absorption properties

The optical and electro-optical absorption spectra, $\varepsilon/\tilde{\nu}$ and $L\varepsilon/\tilde{\nu}$, respectively, are shown in Figs. 2–4, where $\varepsilon^E(\phi,\tilde{\nu})$ is the molar decadic absorption coefficient of the solution in an externally applied electric field, $\tilde{\nu}$ is the wavenumber and ϕ is the angle of light polarization. L is a coefficient denoting the absorption maxima dependence on the applied electric field [30,31] according to Eq. (7)

$$\varepsilon^E(\phi,\tilde{\nu}) = \varepsilon(\tilde{\nu})[1 + L(\phi,\tilde{\nu})E^2 + \cdots] \quad (7)$$

The EOA spectra of **3a–f** are very similar in appearance to the corresponding optical spectra. However, in comparison with the optical absorption maxima, we observe a hypsochromic shift of the electro-optical absorption maxima for parallel polarization ($\phi = 0°$, Figs. 2–4). This shift can be referred to as Stark effect; it indicates the negative difference between the ground- and excited-state dipole

Table 1
Molecular parameters[a], optical[b] and electrical[c] properties of chromophores **3a–f** and *p*-nitroaniline (**pNA**)[d] from UV–vis and EOA measurements

Compound	**3a**	**3b**	**3c**	**3d**	**3e**	**3f**	**pNA**
M	218.21	189.17	231.25	175.14	279.25	200.15	138.12
M.p.	665–668[e]	478–481[e]	496–502	557–563	593–595[e]	559–563[e]	–
λ_{ag}	372	374	375	392	419	441	354
	(362)	(358)	–	(360)	(396)	(419)	–
μ_{ag}	23.9[f]	18.1[f]	17.6	16.8[f]	20.2[f]	18.2	16.4
μ_g	43.4	34.9	35.0	33.8	31.2	21.4	20.5
$\Delta\mu_{ag}$	−4.5	−16.1	−15.3	−16.7	−26.8	−18.3	31.3
β_0	−5.05	−10.26	−10.10	−9.27	−26.19	−17.98	16.0

[a] Molecular weight (M) in g mol^{-1}.
[b] UV–vis in 1,4-dioxane and in acetonitrile (in parentheses); absorption maximum (λ_{ag}) in nm and transition dipole moment (μ_{ag}) in 10^{-30} cm.
[c] EOAM in 1,4-dioxane; ground-state dipole moment (μ_g) in 10^{-30} cm, difference between ground- and excited-state dipole moments ($\Delta\mu_{ag}$) in 10^{-30} cm, static hyperpolarizability (β_0) in 10^{-50} C V^{-2} m^3.
[d] Ref. [37].
[e] Decomposition points (m.p.) in K.
[f] Determined from acetonitrile solution.

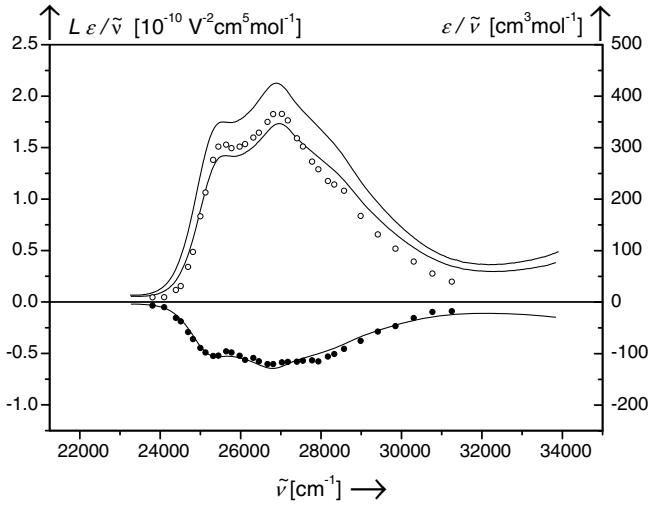

Fig. 2. Optical ($\varepsilon/\tilde{\nu}$, right scale, solid line) and electro-optical ($L\varepsilon/\tilde{\nu}$, left scale; $\phi = 0°$, open circles; $\phi = 90°$, solid circles) absorption spectra of **3a**. Solvent: 1,4-dioxane, $T = 298$ K.

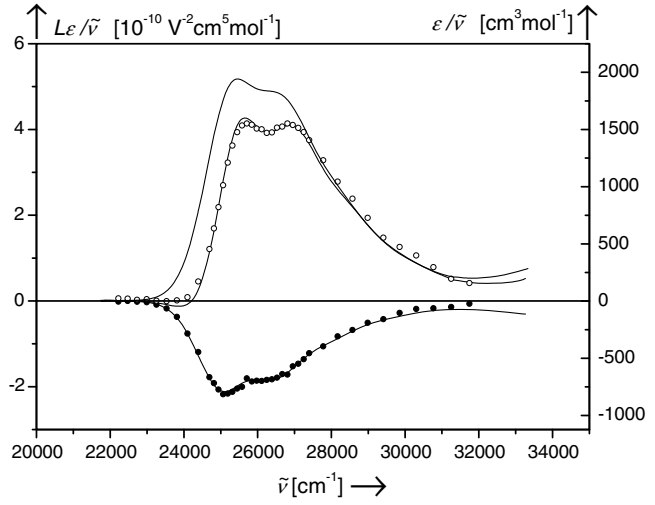

Fig. 3. Optical ($\varepsilon/\tilde{\nu}$, right scale, solid line) and electro-optical ($L\varepsilon/\tilde{\nu}$, left scale; $\phi = 0°$, open circles; $\phi = 90°$, solid circles) absorption spectra of **3d**. Solvent: 1,4-dioxane, $T = 298$ K.

moments $\Delta\mu_{ag}$. The EOA spectra are also characterized by positive electrodichroic effect, *i.e.* increase of the absorption for the parallel polarization of the incident light field relative to the externally applied field and a decrease for the perpendicular polarization ($\phi = 90°$). We attribute this positive electrodichroism to the parallel orientation of the ground-state dipole moment μ_g and the transition dipole moment μ_{ag} as suggested by the C_{2v} symmetry of the molecules.

We have determined the dipole moments in ground and excited states (Table 1) and estimated the values of their static molecular hyperpolarizabilities β_0 according to the equations established by Liptay et al. [30,31].

By varying the substitution nature, the ground-state dipole moments μ_g significantly change decreasing more

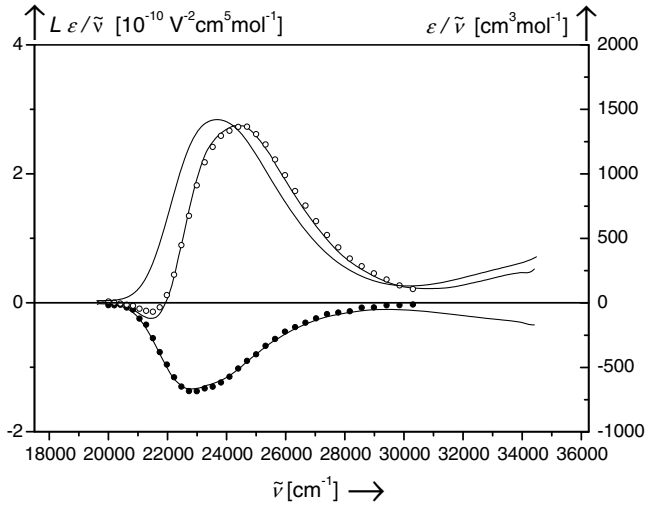

Fig. 4. Optical ($\varepsilon/\tilde{\nu}$, right scale, solid line) and electro-optical ($L\varepsilon/\tilde{\nu}$, left scale; $\phi = 0°$, open circles; $\phi = 90°$, solid circles) absorption spectra of **3e**. Solvent: 1,4-dioxane, $T = 298$ K.

than twice from the most donating (43.4×10^{-30} cm for **3a**) to the most electron withdrawing group (21.4×10^{-30} cm for **3f**). This change results in 70 nm red-shifting of λ_{ag} within the series studied. Moreover, **3f** absorbs at about 90 nm lower wave length as compared to the prototype *p*-nitroaniline. The corresponding molecular parameters for this well known NLO-phore [37] are listed in Table 1 for comparison.

In accordance with their solvatochromic behaviour [19,22]**3a-f** exhibit lower dipole moments in excited state and therefore a less polar structure. The dipole moment of **3a** (with the highest polar ground-state structure) changes only slightly upon excitation and hence its $\Delta\mu_{ag}$ appears much lower than these of the other molecules and particularly than that of *p*-nitroaniline (Table 1). Among the whole series, the two acceptor substituted compounds, 4-COC_6H_5(**3e**) and 4-CN (**3f**), acquire the most favorable $\Delta\mu_{ag}$ values.

The reverse CT upon excitation *i.e.* from the acceptor to the donor group accounts for the negative $\Delta\mu_{ag}$ and therefore negative β_0(exp) of all pyridinium-betaines of squaric acid studied by us so far. Since only the absolute value of β_0(exp) determines the magnitude of the NLO response, the internally charged chromophores discussed here suggest a high potential for NLO applications. Their static hyperpolarizabilities range from -5.05×10^{-50} to -26.19×10^{-50} C V^{-2} m^3 (EOAM). These values are comparable to β_0 of the prototype molecule *p*-nitroaniline [37] and a number of well-known and efficient NLO-phores for electro-optical and photorefractive applications [1,38–41]. The static hyperpolarizabilities depend significantly on the substitutent nature. Their values increase with decreasing donor properties of the substitution in the pyridinium ring. Thus the acceptor substituted **3e** and **3f** show the highest values within the elucidated series. The 4-benzoyl derivative exceeds almost twice the β_0(exp) in the 4-cyano

compound (Table 1). As the chromophore crystallizes in noncentrosymmetric space group due to its Λ-type molecular conformation, this most favourable β_0(exp) is combined with the most favourable bulk properties [22,23].

3.3. Quantum-chemical analysis

To further explore the relationship between the molecular structure and NLO efficiency and in order to explain the observed trends in the nonlinear optical behavior of the studied compounds, we have combined the experimental studies with theoretical predictions. Molecular polarizabilities and hyperpolarizabilities were estimated using the CPHF method. The components of the first molecular hyperpolarizabilities along the dipole axis $\beta_{0,vec}$ and $\beta_{0,tot}$ are identical for **3a–d** and **3f**. Only exception is **3e** for which a small difference of 0.5×10^{-50} C V^{-2} m^3 was calculated. Based on this similarity between $\beta_{0,vec}$ and $\beta_{0,tot}$, we can assume a 1D topology for the whole series of NLO-phores. In this case a two-level approximation appears as the best choice of theoretical model to estimate β. A summary of the calculation results is given in Table 2. Since the variation of $\beta_{0,vec}$ and $\beta_{0,tot}$ is very similar, only the $\beta_{0,vec}$ values are included.

The theoretical calculations also confirm the assumption that the acceptor groups favour the CT excitation. The calculated HOMO–LUMO gaps (Table 2) describe very well the bathochromic shift of the optical absorption maxima observed for the chromophores (Table 1). In the theoretical model the replacement of a donor group with an acceptor group in the pyridinium ring lowers both the HOMO and the LUMO energy but the change in the LUMO energy is greater and this causes smaller HOMO–LUMO gaps and the observed red-shifting.

Although the DFT calculations tend to overestimate the ground-state dipole moments, the variation of μ_g^{calc} is in good agreement with the experimentally determined decrease of the ground-state dipole moments.

In order to illustrate the CT in ground state, we have calculated the natural bond orbital (NBO) atomic charges of studied species from their optimized B3LYP/6-311G** geometry and summarized them over fragments as shown in Table 3. The molecules were regarded as constituted of three fragments – cyclobutenedione moiety (Sq), pyridinium ring (Py) and substituent (R). The substituent is expected to increase or decrease the donor properties of the pyridinium ring by its own electron releasing or withdrawing ability and thus to influence the CT in the molecule.

Table 3
Theoretically calculated NBO (B3LYP/6-311G**) charges over fragments of **3a–f**

Compound	Sq	Py	R
3a	−0.562	0.492	0.070
3b	−0.491	0.427	0.065
3c	−0.496	0.429	0.067
3d	−0.470	0.470	–
3e	−0.417	0.391	0.046
3f	−0.401	0.388	0.013

The excellent acceptor properties of the squaric fragment are revealed by the complete localization of the negative charge over this fragment, even in the presence of cyano or benzoyl group in the pyridinium ring. The introduction of donor substituents leads to a larger displacement of electron density from the heterocycle to the squarate fragment which in turn increases the dipole moments in ground state. Given the strong conjugation and the aromatic character of the system, it is not surprising that the substituents releasing or withdrawing electrons through mesomeric effects influence the CT to a larger extend than those acting through inductive effects.

According to the generally accepted views of the CT influence on the first hyperpolarizability [1–5], higher β values should be expected for smaller HOMO–LUMO energy gaps. In general, the decrease of the HOMO–LUMO energy gaps along with the decrease of the ground-state dipole moments are accurately reproduced in the numerical model, *i.e.* the resulting β values are substantially higher for acceptor substituted compounds in comparison with the donor substituted.

Direct comparison between predicted and experimental EOAM values of β is of limited usefulness since the calculations deal with chromophores in gas phase, whereas the EOA measurements were conducted in solvent 1,4-dioxane. Nonetheless, this theoretical method offers a reliable estimation of the general increasing trend of β when an acceptor substituent is introduced. In accordance with the experiment, the theoretical β values (Tables 1 and 2) predict higher NLO efficiency for **3e** and **3f** in comparison with the *p*-nitroaniline. It is of interest to compare not only to the prototype molecule of *p*-nitroaniline, but also to some structurally related compounds as for example, squaric acid and 3-methyl-4-nitropyridine 1-oxide (POM). The pure squaric acid has rather modest performance ($\beta_{0,vec} = 0.8 \times 10^{-50}$ C V^{-2} m^3, calculated at the same level of theory) and even the larger molecule of POM [42] shows NLO activity, comparable only to the least efficient NLO-phore **3a** in the series reported here. Thus the conversion of

Table 2
Theoretically calculated[a], ground-state moments (μ_g^{calc})[b], linear static polarizability (α)[c], static hyperpolarizabilities ($\beta_{0,vec}$)[d] and HOMO–LUMO energy band gap (ΔE)[e] of **3a–f**

Compound	**3a**	**3b**	**3c**	**3d**	**3e**	**3f**	**pNA**
μ_g^{calc}	52.1	40.3	42.2	38.0	35.5	19.1	25.7
α	20.78	20.82	26.68	18.60	27.64	23.32	18.60
$\beta_{0,vec}$	1.75	5.67	6.25	5.43	15.47	11.5	5.99
ΔE	2.69	2.42	2.44	2.37	2.04	1.95	4.20

[a] Calculations at B3LYP/6-311G** level.
[b] μ_g^{calc} in 10^{-30} cm.
[c] α in 10^{-40} C V^{-1} m^2.
[d] $\beta_{0,vec}$ in 10^{-50} C V^{-2} m^3.
[e] ΔE in eV.

the squaric acid into corresponding pyridinium-betaines is a way to improve the CT and to enhance the molecular NLO response of these species. Computational studies on other chromophores [41–43] have reported similar static hyperpolarizabilities for aromatic systems and possible enhancement of β related to the increased polarity of the surrounding medium or phototriggered properties.

The high molecular hyperpolarizability is not the only desirable property for new organic NLO materials; sufficient thermal stability and crystal packing effects have to be taken into account as well in the experimental [44,45] and theoretical investigations [46].

3.4. Structural characterization in solid state

In all studied structures the molecules are connected trough non-classical C–H···O hydrogen bonds and $\pi\cdots\pi$ interactions between the oppositely charged Sq and Py fragments [23–28]. The squarate carbonyl O atom usually forms a bifurcated hydrogen bond.

Species **3a** and **3d** crystallize in monoclinic ($P2_1/m$) and orthorhombic ($Pcnb$) space groups respectively. The high polarity of these pyridinium-betaines of the squaric acid causes formation of pairs of molecules with antiparallel orientation in the crystal. Both structures are centrosymmetric *i.e.* they are not expected to show macro second-order NLO response.

Due to its lower polarity and the non-planar molecular structure (Λ-type molecular conformation) **3e** crystallizes noncentrosymmetrically in orthorhombic space group $Pna2_1$. The unit cell consists in four molecules, with antiparallel stacking. This arrangement is not optimal for a high bulk optical nonlinearity, since the dipole–dipole electrostatic interaction reduces the overall NLO response. However, it deserves attention as the first reported noncentrosymmetric crystal structure of this class of compounds. Moreover, often different polymorphic forms are observed for one compound and better arrangement in the crystal structure could be achieved in this way [44].

3.5. Thermogravimetric analysis

Due to the large networks of weak but numerous intermolecular non-classical hydrogen bonds which stabilize the three-dimensional packing of the crystals, the squaric acid derivatives of **3a–f** type decompose more often than melt (Table 1). In both cases it is above 470 K (near 670 K for the crystal of **3a**).

The TG–DTG data for **3c** (recrystallized from ethanol), **3d** (recrystallized from water), **3e** (not recrystallized sample) and **3f** (recrystallized from glacial acetic acid) are presented in Figs. 5 and 6.

For all samples a sharp fall in the TG curve (about 65% wt.) characterized by a well-defined maximum in the DTG profile is observed in the interval 575–592 K (Figs. 5 and 6a), indicating that decomposition process occurred. In the lower temperature region no or only a very slight effect

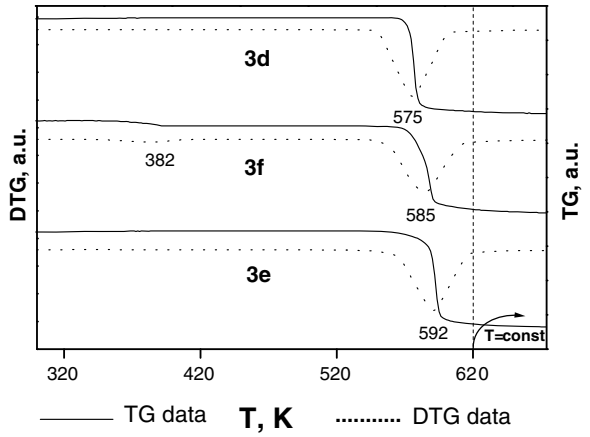

Fig. 5. TG (solid line) and DTG (dotted line) data of the squaric acid derivatives **3d–f**.

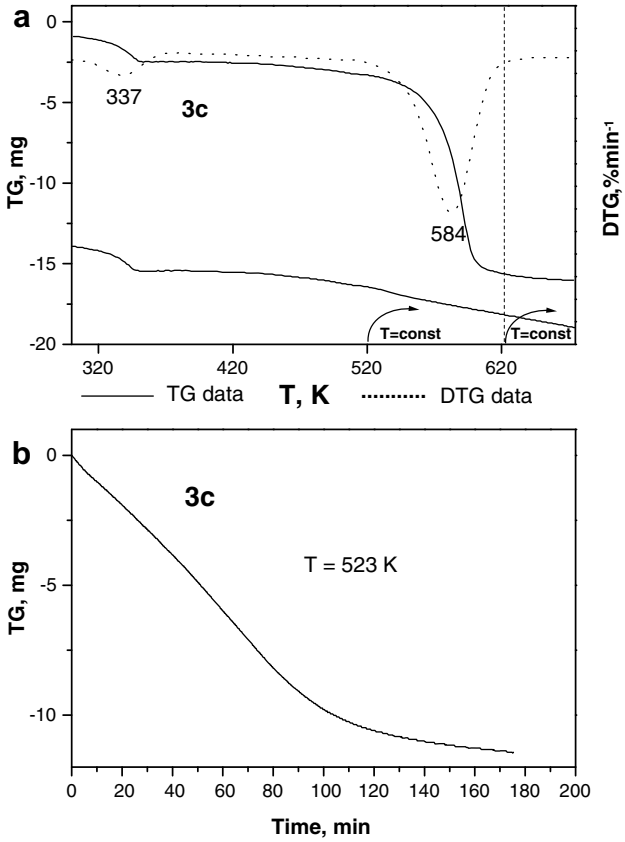

Fig. 6. TG (solid line) and DTG (dotted line) data of **3c** squaric acid derivative versus temperature (a) and versus time (b). The time dependent measurement was carried out at 523 K.

(at 382 K for **3f**, Fig. 5; 337 K for **3c**, Fig. 6) was found. They are due to the escape of physisorbed acetic acid from **3f** (Fig. 5) and ethanol in the case of **3c** (Fig. 6a). The shifting of the DTG maximum to higher temperatures indicates an increase in the stability of the squaric acid derivatives in the following order: **3d** < **3c** ≅ **3f** < **3e**. The two acceptor substituted compounds **3e** and **3f** show remarkable thermal

stability which is much higher than the typical for organic NLO molecular crystals [38–41]. In addition, **3e** and **3f** are the most NLO active within the investigated series. These two characteristics give them advantage for application in NLO devices as well as motivate further design of new NLO materials based on acceptor substituted pyridinium-betaines of squaric acid.

For the donor substituted **3c** the TG curve starts to decrease at about 440 K (Fig. 6a). This temperature is considerably lower than the decomposition temperature of 584 K (Fig. 6a). The observed effect is due to the initial melting of the sample, also confirmed by a melting point determination (see Table 1). The large difference between melting and decomposition temperature favors the formation of single crystalline thin films by applying melt-growth techniques [44]. In order to monitor the thermal stability of **3c** in melt, we have conducted a second experiment with the sample being kept for ca 3 h at 523 K, *i.e.* 20 K above its melting point (Fig. 6b). At this temperature **3c** comprises a melt that slowly sublimates. The weight loss is nearly constant with the time. Within the first 100 min the sample looses about 47% of its weight (Fig. 6b). After that the sublimation considerably decreases due to the depletion of the sample's substance. Here only about 7% of weight loss was registered after 70 min at 523 K. Hence, in this time interval (after 100 min) the **3c** derivative represents a stable melt and appears to be suitable for growing crystals by melt-growth technique, a method offering great prospectives as recently demonstrated by [44].

4. Conclusions

A combined experimental and theoretical study on the molecular NLO efficiency and the bulk crystal thermal properties of a series of squaric acid based chromophores was carried out. The chromophores exhibit high hyperpolarizabilities (-5.05 to -26.19×10^{-50} C V^{-2} m^3) which depend strongly on the nature of the substituents. Based on the experimentally and theoretically derived correlation between the donor–acceptor substitution and the hyperpolarizability's magnitude, the synthesis of acceptor-substituted, and more particularly carbonyl-substituted, pyridinium-betaines of squaric acid was outlined as successful strategy for the design of new efficient organic NLO-phores. The thermal stability and high decomposition points observed for the crystals of **3a–f** give them another advantage for application as single-crystal NLO materials. Although the greater part of the studied crystalline samples decompose, there are also melting substances among them – the alkyl-substituted **3b** and **3c**. **3c** represents a stable melt over a long period of time and therefore crystals of the alkyl-substituted derivatives could be grown using melt-growth techniques. Finally, **3e** combines the most favorable properties – the highest β value, great thermal stability and noncentrosymmetic crystal structure which make it the most attractive among the series for second-order NLO applications.

Acknowledgements

T.K. and D.Y. thank to Alexander von Humboldt Foundation, DAAD (grant within the priority program "Stability Pact for South-Eastern Europe"), and Bulgarian National Science Fund (Contract X-1510).

References

[1] J. Wolff, R. Wortmann, Adv. Phys. Org. Chem. 32 (1999) 121.
[2] H. Nalwa, S. Miyata, in: H. Nalwa, S. Miyata (Eds.), Nonlinear Optics of Organic Molecules and Polymers, CRC Press, Inc., Boca Ratton, 1997, Chapter 4.
[3] H.S. Nalwa, T. Watanabe, S. Miyata, Opt. Mater. 2 (1993) 73.
[4] B. Champagne, D. Bishop, Adv. Chem. Phys. 126 (2003) 41.
[5] M. Yang, B. Champagne, J. Phys. Chem. A 107 (2003) 3942.
[6] D.F. Aeton, Science 253 (1991) 281.
[7] S. Gilmour, R.A. Montgomery, S.R. Marder, L.T. Cheng, A.K.-Y. Jen, Y. Cai, J.W. Perry, L.R. Dalton, Chem. Mater. 6 (1994) 1603.
[8] D.M. Burland, R.D. Miller, C.A. Walsh, Chem. Rev. 94 (1994) 31.
[9] T.J. Marks, M.A. Ratner, Angew. Chem. Int. Ed. Engl. 34 (1995) 155.
[10] W. Lin, S. Yitzchaik, A. Malik, M.K. Durbin, A.G. Richter, G.K. Wong, P. Dutta, T.J. Marks, Angew. Chem. Int. Ed. Engl. 34 (1995) 1497.
[11] T. Yamashiki, S. Fukuda, K. Tsuda, T. Gotoh, Appl. Phys. Lett. 83 (2003) 605.
[12] X. Zheng, S. Wu, R. Sobolewski, R. Adam, M. Mikulics, P. Kordoš, M. Siegel, Appl. Phys. Lett. 82 (2003) 2383.
[13] M. Sliwa, S. Letard, I. Malfant, M. Nierlich, P.G. Lacroix, T. Asahi, H. Masuhara, P. Yu, K. Nakatani, Chem. Mater. 17 (2005) 4727.
[14] L. Pu, Nonlinear Opt. 3 (1992) 233.
[15] R. Bonnett, M. Motevalli, J. Siu, Tetrahedron 60 (2004) 8913.
[16] M. Yang, Y. Jiang, Chem. Phys. 274 (2001) 121.
[17] U. Lowrentz, W. Grahn, I.P.G. Jones, Acta Crystallogr., C 57 (2001) 126.
[18] A. Feldner, D. Scherer, M. Welscher, T. Vogtmann, M. Schwoerer, U. Lawrentz, T. Laue, H.H. Johannes, W. Grahn, Nonlinear Opt. 26 (2000) 99.
[19] T.M. Kolev, D.Y. Yancheva, S.I. Stoyanov, Adv. Funct. Mater. 14 (2004) 799.
[20] T.M. Kolev, D.Y. Yancheva, B.A. Stamboliyska, Spectrochim. Acta 59 (2003) 1805.
[21] T.M. Kolev, B.A. Stamboliyska, D.Y. Yancheva, V. Enchev, J. Mol. Struct. 191 (2004) 241.
[22] T. Kolev, B. Stamboliyska, D. Yancheva, Chem. Phys. 324 (2006) 489.
[23] T. Kolev, D. Yancheva, D.C. Kleb, M. Schurmann, H. Preut, P. Bleckmann, Z. Kristallogr. – New Cryst. Struct. 216 (2001) 65.
[24] T. Kolev, D. Yancheva, M. Schurmann, D.C. Kleb, H. Preut, M. Spiteller, Acta Crystallogr., E 58 (2002) o1267.
[25] T. Kolev, R. Wortmann, M. Spiteller, W.S. Sheldrick, H. Mayer-Figge, Acta Crystallogr., E 60 (2004) o1449.
[26] T. Kolev, D. Yancheva, B. Shivachev, R. Petrova, M. Spiteller, Acta Crystallogr., C 61 (2005) o213.
[27] T. Kolev, R. Wortmann, M. Spiteller, W.S. Sheldrick, H. Meyer-Figge, Acta Crystallogr., E 61 (2005) o1090.
[28] T. Kolev, D. Yancheva, B. Shivachev, R. Petrova, Acta Crystallogr., E 63 (2007) o3259.
[29] A. Schmidt, U. Becker, A. Aimene, Tetrahedron Lett. 25 (1984) 4475.
[30] W. Liptay, E.C. Lim (Eds.), Excited States, Dipole Moments and Polarizabilities of Molecules in Excited Electronic States, vol. 1, Academic Press, New York, 1974, p. 129.
[31] R. Wortmann, K. Elich, S. Lebus, W. Liptay, P. Borowicz, A. Grabowska, J. Chem. Phys. 96 (1992) 9724.
[32] M.J. Frisch, G.W. Trucks, H.B. Schlegel, G.E. Scuseria, M.A. Robb, J.R. Cheeseman, V.G. Zakrzewski, J.A. Montgomery Jr., R.E.

Stratmann, J.C. Burant, S. Dapprich, J.M. Millam, A.D. Daniels, K.N. Kudin, M.C. Strain, O. Farkas, J. Tomasi, V. Barone, M. Cossi, R. Cammi, B. Mennucci, C. Pomelli, C. Adamo, S. Clifford, J. Ochterski, G.A. Petersson, P.Y. Ayala, Q. Cui, K. Morokuma, D.K. Malick, A.D. Rabuck, K. Raghavachari, J.B. Foresman, J. Cioslowski, J.V. Ortiz, A.G. Baboul, B.B. Stefanov, G. Liu, A. Liashenko, P. Piskorz, I. Komaromi, R. Gomperts, R.L. Martin, D.J. Fox, T. Keith, M.A. Al-Laham, C.Y. Peng, A. Nanayakkara, C. Gonzalez, M. Challacombe, P.M.W. Gill, B. Johnson, W. Chen, M.W. Wong, J.L. Andres, C. Gonzalez, M. Head-Gordon, E.S. Replogle and J.A. Pople, Gaussian 98, Revision A.7, Gaussian, Inc., Pittsburgh, PA, 1998.

[33] D. Becke, J. Chem. Phys. 98 (1993) 5648.

[34] C. Lee, W. Yang, R.G. Parr, Phys. Rev. B 37 (1988) 785.

[35] A. Willetts, J.E. Rice, D.A. Burland, D.P. Shelton, J. Chem. Phys. 97 (1992) 7590.

[36] T. Kolev, B. Koleva, M. Spiteller, H. Mayer-Figge, W.S. Sheldrick, J. Phys. Chem. 111 (2007) 10084.

[37] R. Wortmann, P. Krämer, C. Glania, S. Lebus, N. Detzer, Chem. Phys. 173 (1993) 99.

[38] R. Wortmann, C. Glania, P. Krämer, K. Lukaszuk, R. Matschiner, R.J. Twieg, F. You, Chem. Phys. 245 (1999) 107.

[39] F. Würthner, R. Wortmann, R. Matschiner, K. Lukaszuk, K. Meerholz, Y. DeNardin, R. Bittner, C. Bräuchle, R. Sens, Angew. Chem. Int. Ed. Engl. 36 (1997) 2765.

[40] C. Peng, P.Y. Ayala, H.B. Schlegel, M.J. Frisch, J. Comput. Chem. 17 (1996) 49.

[41] G. Archetti, A. Abbotto, R. Wortmann, Chem. Eur. J. 12 (2006) 7151.

[42] B. Champagne, E.A. Perpète, T. Legrand, D. Jacquemin, J.-M. André, J. Chem. Soc., Faraday Trans. 94 (1998) 1547.

[43] L. Sanguinet, J.L. Pozzo, V. Rodrigez, F. Adamietz, F. Castet, L. Ducasse, B. Champagne, J. Phys. Chem. B 109 (2005) 11139.

[44] O.P. Kwon, B. Ruiz, A. Choubey, L. Mutter, A. Schneider, M. Jazbinsec, V. Gramlich, P. Günter, Chem. Mater. 18 (2006) 4049.

[45] O.P. Kwon, S.J. Kwon, M. Jazbinsec, A. Choubey, L. Mutter, A. Schneider, V. Gramlich, P. Günter, Adv. Funct. Mater. 17 (2007) 1750.

[46] M. Guillaume, E. Botek, B. Champagne, J. Chem. Phys. 121 (2004) 7390.